First observation of the β decay of neutron-rich ^{218}Bi by the pulsed-release technique and resonant laser ionization

H. De Witte,[1] A. N. Andreyev,[2] I. N. Borzov,[3] E. Caurier,[4] J. Cederkäll,[5] A. De Smet,[1] S. Eeckhaudt,[1,*] D. V. Fedorov,[6] V. N. Fedosseev,[5] S. Franchoo,[5,7,†] M. Górska,[1,‡] H. Grawe,[8] G. Huber,[7] M. Huyse,[1] Z. Janas,[9] U. Köster,[5] W. Kurcewicz,[9] J. Kurpeta,[9] A. Płochocki,[9] K. Van de Vel,[1] P. Van Duppen,[1] and L. Weissman[5,§]

[1]*University of Leuven, B-3001 Leuven, Belgium*
[2]*University of Liverpool, Liverpool L697ZE, United Kingdom*
[3]*Université Libre de Bruxelles, B-1050 Brussels, Belgium*
[4]*Institut de Recherches Subatomiques, F-67037 Strasbourg, France*
[5]*CERN ISOLDE, CH-1211 Genève 23, Switzerland*
[6]*Petersburg Nuclear Physics Institute, RU-188350 Gatchina, Russia*
[7]*University of Mainz, D-55099 Mainz, Germany*
[8]*GSI, D-64291 Darmstadt, Germany*
[9]*University of Warsaw, PL-00681 Warsaw, Poland*

The neutron-rich isotope ^{218}Bi has been produced in proton-induced spallation of a uranium carbide target at the ISOLDE facility at CERN, extracted from the ion source by the pulsed-release technique and resonant laser ionization, and its β decay is studied for the first time. A half-life of 33(1)s was measured and is discussed in the self-consistent continuum-quasi particle-random-phase approximation framework that includes Gamow-Teller and first-forbidden transitions. A level scheme was constructed for ^{218}Po, and a deexcitation pattern of stretched $E2$ transitions $8^+ \rightarrow 6^+ \rightarrow 4^+ \rightarrow 2^+ \rightarrow 0^+$ to the ground state is suggested. Shell-model calculations based on the Kuo-Herling interaction reproduce the experimental results satisfactorily.

I. INTRODUCTION

The neutron-rich lead region is of exceptional interest to trace the evolution of single-particle levels and the residual proton-neutron interaction beyond the doubly magic nucleus ^{208}Pb. While ^{208}Pb is well understood in terms of the shell model, experimental data on the heavier isotopes are very scarce and it is far from clear to what extent the shell model is upheld [1]. In particular, extended systematics have been collected over the past years for the neutron-deficient polonium isotopes down to ^{190}Po [2–4] but it remains an open question how the structure evolves on the neutron-rich side, where protons occupy the $f_{7/2}$ and $h_{9/2}$ and neutrons the $g_{9/2}$ orbitals.

In the present paper we focus on the decay of ^{218}Bi to ^{218}Po. In the latter nucleus, only a γ ray of 510(2)keV was known from the α decay of ^{222}Rn [5], tentatively assigned to the deexcitation of the first 2^+ level. The scarcity of data follows from the mass contaminations that β-decay studies at on-line mass separators often suffer from [6]. On the other hand, at the FRS facility at GSI reaction products were identified in the fragmentation of a ^{238}U beam at 1000 MeV per nucleon up to ^{212}Tl, ^{215}Pb, ^{218}Bi, and ^{220}Po. Due to the low yields, however, spectroscopic information in the heavier nuclei could only be obtained for microsecond isomers in ^{208,212}Pb and ^{210,211}Bi [7].

In a simple and elegant way, the pulsed-release technique allows us to considerably reduce the contamination at on-line mass separators on the condition that the isotopes of interest are longer lived than the unwanted species [8]. In the mass region $215 < A < 219$, this indeed holds for the β-decaying lead and bismuth isotopes versus the francium α emitters. In an earlier experiment, new spectroscopic data were thus obtained in the $A = 215, 216, 217$ isobaric chains [9–11]. In the current experiment we have complemented the pulsed-release suppression of contaminants with the element selectivity of the RILIS laser ion source at ISOLDE [12,13]. By comparing spectra that are taken with and without laser irradiation of the ion source, the unique signature of the element under investigation becomes evident. Our paper details the findings for ^{218}Bi, the β decay of which has been observed for the first time, while the results obtained in the $A = 215$ chain will be published elsewhere [14,15].

II. EXPERIMENTAL SETUP

The experiment was carried out at the General Purpose Separator of the ISOLDE facility at CERN, Geneva. A 1.4 GeV pulsed proton beam was delivered by the PS Booster to a UC$_x$ graphite target of 50 g/cm^2 thickness. Out of the 14 proton pulses that are contained in every PS-Booster supercycle and which are 1.2 s apart, 10 were sent to ISOLDE. The intensity was on average 3×10^{13} protons per pulse.

*Present address: University of Jyväskyä, FIN-40351 Jyväskylä, Finland.

†Corresponding author. Email address: serge.franchoo@cern.ch

‡Present address: GSI, D-64291 Darmstadt, Germany.

§Present address: Michigan State University, East Lansing, MI 48824.

The ions diffused out of the target into the ion-source cavity, which consisted of a niobium tube of 30 mm long with an internal diameter of 3 mm. Resonant laser ionization of bismuth in the cavity was accomplished in three steps [12]. A first tunable pulsed dye laser with wavelength λ_1 = 306.8 nm and 10 mW power lifted the atom from the $6p^3$ $^4S^0_{3/2}$ ground state to the $6p^27s$ $^4P_{1/2}$ excited state. The ultraviolet radiation was obtained by doubling the fundamental frequency with a nonlinear beta barium borate crystal. A second identical laser with λ_2 = 555.2 nm and 120 mW power provided the necessary energy for the atomic transition to the $6p^28p[1]^0_{3/2}$ level. Both dye lasers were pumped by copper-vapor lasers, operating at a repetition rate of 11 kHz. The latter at the same time supplied the energy for the final ionizing transitions to the continuum at $\lambda_{3,1}$ = 510.6 nm and $\lambda_{3,2}$ = 578.2 nm, with 1900 mW of power.

The off-line ionization efficiency for bismuth was determined to be 6% [12]. However, during the actual experiment the laser power in the last step was twice lower than off-line and an efficiency of 3% can be estimated. The linewidth of the dye-laser radiation covered about 10 GHz. Albeit broad, the wavelength of the first-step laser nevertheless had to be corrected for the atomic hyperfine splitting and isotope shift.

The extracted ions were subsequently mass separated. During our measurements, the separator remained closed for an extended span of 20 ms after the impact of the proton beam on the target. This way of operation is known as the pulsed-release technique [8] and enabled the efficient suppression of short-lived isobaric contaminants, in particular surface-ionized francium.

The ions were finally implanted in an aluminized Mylar tape, 100 μm thick and 12.5 mm wide. The transmission efficiency from the focal plane of the separator to the tape was 85(2)%. After collection, the sample was transported to the detection setup every ten supercycles, i.e., 168 s. The setup consisted of two high-purity germanium detectors of 70% and 75% relative efficiency, one low-energy germanium detector with a 0.3 mm thin beryllium entrance window, and an NE102A plastic scintillator in front of the latter. The scintillator had a thickness of 1 mm and a surface of 31 $\times 25$ mm^2. All detectors were arranged in close geometry. The data were recorded as $\beta X\gamma\gamma$ coincidences with an MBS-based acquisition system. Any two detectors firing simultaneously triggered the acquisition.

III. RESULTS

Comparison of the β-gated γ spectra collected with and without laser irradiation of the ion source allowed to unambiguously identify the γ deexcitation pattern that can be ascribed to the β decay of ^{218}Bi. These spectra are shown in Fig. 1. The measurement times with and without laser irradiation were 325 and 9 min, respectively. The spectra contain contaminant lines from ^{208}Tl, a product of the decay of ^{220}Fr, while also ^{84m}Br can be seen, most likely separated in the form of molecular BaBr after bonds with stable barium impurities in the target material.

In as far as the statistics allowed, it was cross checked that the newly found lines were coincident with atomic polonium
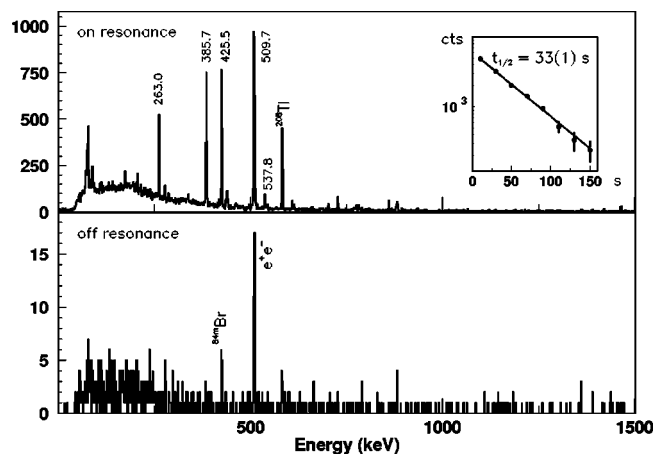

FIG. 1. β-gated γ spectrum at mass 218 with (top) and without (bottom) laser irradiation of the ion source. The lines of which the energy is given (in keV) are attributed to the decay of ^{218}Bi. The inset shows the half-life behavior of the sum of the 263.0 and 385.7 keV transitions together with a single exponential fit.

x rays. The energies and the relative intensities of the γ rays that we assign to the decay of ^{218}Bi are listed in Table I. These intensities were divided by the efficiency of the detector setup, determined by means of GEANT simulations [16]. Since the 509.8 keV line overlapped with the annihilation peak and the 425.5 keV line was corrupted by the ^{84m}Br contamination, normalization was performed with respect to the 385.7 keV ray.

An exponential fit of the time behavior of the 385.7 and 263.0 keV γ lines yielded a half-life of 33(1)s. The transitions at 425.5 and 509.8 keV could not be used as they were contaminated by ^{84m}Br activity and annihilation radiation, respectively. In as far as the statistics were sufficient, the remaining lines that are attributed to the decay of ^{218}Bi

TABLE I. γ-ray energies E, coincidence relations, and relative intensities $\dagger_\gamma$ of γ rays assigned to the decay of ^{218}Bi.

| E (keV)	coincident lines	$\dagger_\gamma$(%)
174.5(9)	263.0, 385.7, 425.5, 509.7	<2.2
176.6(9)	263.0, 385.7, 425.5, 509.7	<1.3
263.0(1)	174.5, 176.6, 287.1, 385.7, 418.3, 425.5, 463.5, 509.7, 702.9	59(16)
287.1(2)	176.6, 263.0, 385.7, 425.5, 509.7	<2.7
385.7(1)	174.5, 263.0, 287.1, 418.3, 425.5, 437.0, 463.5, 509.7, 537.8, 702.9	100.0
418.3(5)	263.0, 425.5, 509.7	6(2)
425.5(1)	174.5, 176.6, 263.0, 287.1, 385.7, 437.0, 463.5, 509.7, 537.8	95(27)
437.0(2)	385.7, 425.5, 509.7	4(2)
463.5(6)	385.7, 425.5, 509.7	6(2)
509.7(1)	174.5, 176.6, 263.0, 287.1, 385.7, 425.5, 437.0, 463.5, 537.8	134(42)
537.8(1)	385.7, 425.5, 509.7	12(3)
702.9(3)	263.0, 385.7, 509.7	7(3)
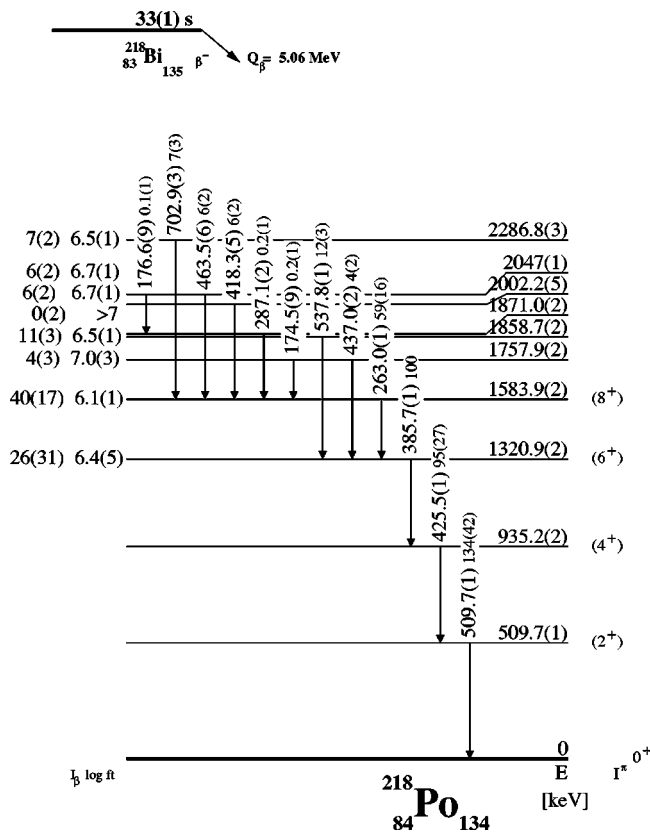
FIG. 2. Proposed level scheme of ^{218}Po. The log ft values are lower limits as γ rays from higher levels can have escaped detection.

Taking into account a transmission ratio from the focal plane of the separator to the detector setup of 85(2)% as quoted before, the simulated efficiency of the setup, and adopting a branching ratio of 100 % for the 425.5 keV ray, the production rate of ^{218}Bi was determined at 44(8) at/μC. This number includes a correction for γ summing, conversion, the fraction of the activity removed by the tape before having decayed, and the fraction not released from the ion source due to the period of 20 ms the separator being closed after impact of the proton beam, as explained above.

showed consistent half-lives, albeit somewhat longer, due to underlying Compton events from the contaminations.

A γ-γ coincidence matrix was constructed, the relations of which are printed in Table I. For that matter, the table includes a number of weaker transitions that became apparent from the coincidence spectra only. From the coincidence relations it was deduced that the four γ rays at 509.8, 425.5, 385.7, and 263.0 keV are in cascade. The 509.8 keV line, since it was known previously from the α decay of ^{222}Rn [5], we place at the bottom. On the basis of systematics, the three remaining lines are placed on top of each other in decreasing energy order and we put forward an $E2$ spin sequence for the cascade of 8^+ down to 0^+.

The level scheme is depicted in Fig. 2. Within the error bars, the intensity of the 425.5 keV line is equal to that of the 385.7 keV transition. Hence there is no direct β feeding to the level at 935.2 keV. The observed feeding pattern to the higher-lying 6^+ and 8^+ states, together with the absence of β decay to the 935.2 keV 4^+ level, renders feeding to the 2^+ level at 509.7 keV unlikely. The large uncertainty in the intensity deexciting this state, due to the contamination of the peak, is consistent with this assessment. Theoretical $E2$ conversion coefficients were used for the four γ transitions in the $8^+ \to 0^+$ cascade to determine the β feeding to the remaining levels and calculate the log ft values.

One may add that we have no experimental evidence for the existence of a β-decaying low-spin isomeric state in ^{218}Bi that would decay to a 2^+ daughter level, as observed in ^{216}Bi [6].

IV. HALF-LIFE CALCULATIONS

The measurement of β-decay half-lives in the $N=126$ region is of importance for nucleosynthesis in order to define the dynamical time scale of the r process. The ratio of the half-lives for β decay and charged-current neutrino capture gives a rigid constraint on the neutrino flux in the most recent neutrino-driven wind scenario of the r process, which includes neutrino flavor oscillations [17]. However, near the r process paths from $Z\approx 60$ to $Z\approx 90$ and $N=126$ the various global models encounter difficulties as not only the Gamow-Teller (GT) but also the first-forbidden (FF) decays are expected to play a role [18]. The self-consistent treatments of β-decay half-lives are of special interest, as they are more reliably extrapolated to regions far from stability and carry the advantage that the predictions of β-decay rates are based on the same ground-state description as the one to calculate the nuclear masses.

We follow the approach to the GT and FF decays which is developed in Ref. [18]. It is based on the self-consistent description of ground states in the framework of the energy-density-functional theory using the Fayans local-density functional DF3 [19]. The β-decay strength functions are calculated in the continuum-quasiparticle-random-phase-approximation-like (QRPA-like) framework of the finite Fermi-system theory (FFS) [20].

The method is free of particle-hole (p-h) basis restrictions. This allows us to adopt the mass-independent, effective NN interaction of the FFS, as well as the mass and energy-independent quenching $Q=g_A/g_V\approx 0.8$–0.9 of the relevant spin-isospin responses in the nuclear medium. The p-h spin-isospin effective NN interaction includes the zero-range repulsion with the Landau-Migdal constant and the finite-range attraction due to the medium-renormalized π and ρ exchanges. The strength parameters are extracted from the experimental position of the giant GT resonance in the single nucleus ^{208}Pb. The particle-particle (p-p) effective NN interaction, i.e., unlike particle or p-n $T=0$ pairing, is used in a form similar to the $T=1$, i.e., like-particle, pairing interaction. Although the $T=1$ pairing interaction is already included at the BCS level, the $T=0$ p-n attraction cannot be omitted as this would destroy the O(8) symmetry of the QRPA equations. The strength of the p-p effective NN interaction, as found from microscopic calculations [21], corresponds to an appreciable reduction of the β^- decay half-lives. Any local fitting of the p-h and p-p effective interactions to the experimentally known β-decay half-lives is thus avoided.

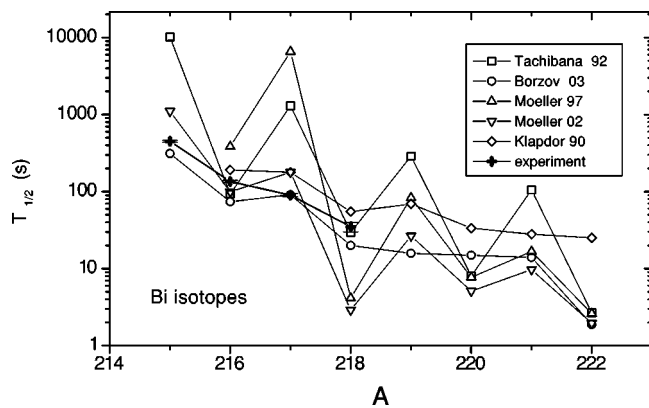FIG. 3. β-decay half-lives of bismuth isotopes predicted by different models [18,22–25] and compared with experimental data taken from Refs. [6,9,10] and the present measurements.

The GT and FF decays are coherently treated within a single microscopic framework.

In Fig. 3 we compare the experimental half-lives of $^{215-217}$Bi [6,9,10], together with our value for ^{218}Bi, with the predictions from the global approaches for $^{215-222}$Bi [18,22–25]. The total half-lives of the GT decay calculated within the finite range droplet model with random phase approximation (FRDM+RPA) model [22] overestimate the experimental ones by orders of magnitude. The scale of the predicted odd-even effects is generally too large because of spurious effects caused by the omission of the *p-p* effective *NN* interaction.

In the recent microstatistical version of the FRDM model [23], the gross-theory calculation of the FF decay is combined with the FRDM + RPA description of the GT decay. This model provides shorter total half-lives than the ones calculated for the GT decay in Ref. [22]. However, the strong renormalization of the GT half-lives, for example, in ^{215,217}Bi, is hard to explain from microscopic arguments. It may well come from the inconsistency in the microstatistical and gross-theory inputs, which is unavoidable in hybrid models.

In the QRPA calculations from Ref. [24], the strengths of the separable *p-h* and *p-p* *NN* interactions are directly fitted to the experimentally known half-lives for every isotopic chain, which is a purely empirical procedure. On the other hand, as the odd-even behavior of the calculated half-lives is reasonable, having included the $T=0$ pairing, such a procedure may in some cases give a sound extrapolation to the closest experimentally unknown nuclei. However, as the FF transitions are not included, it is quite natural that the experimental half-lives of the bismuth isotopes are overestimated.

The results of the gross-theory statistical calculations with a parametric description of the forbidden transitions [25] vary significantly from the odd to the even nuclei.

While a detailed analysis of the β decays close to ^{208}Pb requires due consideration of the energy dependence of the shape factor, beyond ^{208}Pb an estimate within the ξ approximation is still of interest. Our calculated half-lives show a fairly regular *A* behavior for $^{218-221}$Bi, whereas a shorter half-life of 1.8 s is predicted for ^{222}Bi. The slight underestimation of the experimental total half-lives would become
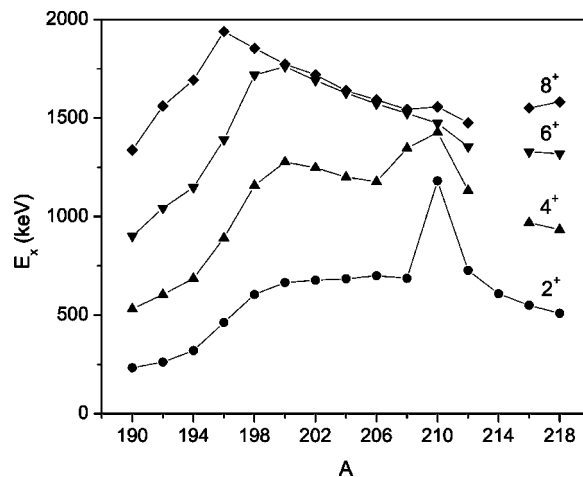

FIG. 4. Evolution of the level structure in polonium isotopes. Data are taken from Refs. [2–4,10,28].

less severe if the quenching factor Q be reduced within its margins of accuracy.

Although our calculations within the same framework and with the same *NN*-interaction parameters show a reasonable agreement with the available experimental data in the $N=50$ and $N=82$ regions [18], the approach may still be too simplified for this particular region east of ^{208}Pb, especially if $\Delta J=0$ transitions dominate the decay schemes. This is mainly due to the neglect of the velocity-dependent terms in the effective *NN* interaction and the use of the Coulomb ξ approximation.

V. SHELL-MODEL CALCULATIONS

In the simplest shell-model configurations for ^{218}Bi the last proton resides in the $f_{7/2}$ or $h_{9/2}$ orbital and the last neutron in $g_{9/2}$ or $i_{11/2}$. For these combinations the ground-state spin can range from 0 to 10. The ground state of ^{218}Po can be conveniently described as a closed core with one additional pair of protons in the $f_{7/2}$ or $h_{9/2}$ orbital and four pairs of neutrons in $g_{9/2}$ or $i_{11/2}$. The easiest way to create excitations in the daughter nucleus consists in aligning the spins of the valence pairs. The observed sequence of the 509.8, 425.5, 385.7, and 263.0 keV transitions could therefore be interpreted as an $E2$ cascade linking 8^+, 6^+, 4^+, and 2^+ levels to the 0^+ ground state of ^{218}Po. This would justify the assumptions in the earlier discussion of the γ intensities and β feeding.

For ^{216}Bi it has been argued that both a longer living state of unknown but low spin and a shorter living 6^-, 7^-, or 9^- high-spin state exist [10]. The high-spin state predominantly feeds the 8^+ level in ^{216}Po. In the case of ^{218}Bi, the distribution of the β strength towards or above the 6^+ and 8^+ levels in ^{218}Po would point to an equal spin of 6^-–9^- for the mother nucleus.

The evolution of the energies of 8^+, 6^+, 4^+, and 2^+ levels in the even-even polonium isotopes is shown in Fig. 4. The lower part of the ^{210}Po level scheme is dominated by the $\pi h_{9/2}^2$ configuration [26]. As neutrons are being added to the nucleus, this structure mostly survives, although mixing with
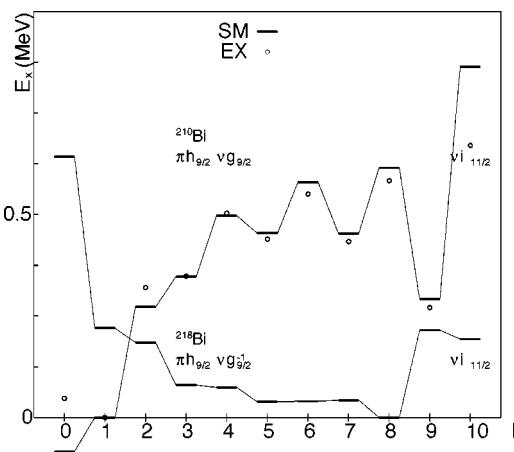
FIG. 5. Calculated and experimental excitation energies of the $\pi h_{9/2}$, $\nu g_{9/2}$, and $\nu i_{11/2}$ multiplets in ^{210}Bi and ^{218}Bi. The circles are experimental data for ^{210}Bi from [28].

other broken valence pairs becomes apparent. The distances among the excited states gradually increase and the 2^+ and 4^+ levels descend. This feature is more pronounced beyond ^{210}Po than below. It should be kept in mind, however, that below ^{210}Po the proton-neutron interaction is small and neutrons can only create low-spin states.

We have used the Kuo-Herling interaction as revised by Warburton and Brown [1] in a model space that includes the $h_{9/2}$, $f_{7/2}$, and $i_{13/2}$ proton orbitals and the $g_{9/2}$, $i_{11/2}$, and $j_{15/2}$ neutron orbitals. No low-spin states were regarded. Single-particle energies were taken from ^{209}Bi and ^{209}Pb and calculations performed with the NATHAN code [27]. Seniority truncation was used, i.e., successively more pairs were allowed to be broken. The number of broken pairs C ranged from 1 to 4. For instance, in the case of $C=4$ eight particles of the two protons and eight neutrons in ^{218}Po could spread freely over the available orbits.

In Fig. 5 the $\pi h_{9/2} \nu g_{9/2}$ odd-parity multiplet is shown for ^{218}Bi in comparison to the pure two-particle case of ^{210}Bi. The configurations that we list have a quasiparticle character, due to pair scattering especially to the $\nu i_{11/2}$ state. The 10^- level always belongs to $\pi h_{9/2} \nu i_{11/2}$. The ^{210}Bi spectrum shows the typical uncertainties of the two-body matrix elements.

From the figure one concludes that the shell model prefers a 8^- ground state for ^{218}Bi, with the 5^- to 7^- levels only about 40 keV above. Furthermore it appears that the $\pi h_{9/2} \nu g_{9/2}$ multiplet changes its nature from particle-particle in ^{210}Bi to particle-hole in ^{218}Bi, as shown by the generally convex (respectively concave) behavior of the curves connecting the multiplet energies. Nevertheless, a pure particle-hole configuration is not reached as the odd-even spin staggering is smooth in ^{218}Bi as compared to ^{210}Bi. Interestingly, the 10^- level has come down, which tells us the effective $\nu i_{11/2}$ separation is small and the orbital interacts strongly with the $\nu g_{9/2}$ state through mixing of $\pi h_{9/2} \nu g_{9/2}^{-1}$ with $\pi h_{9/2} \nu i_{11/2}$ as well as the creation of $\nu i_{11/2}$ pairs from $\nu g_{9/2}$ pairs. The calculated multiplet structure does not support the existence of a low-spin isomer, which as mentioned above we indeed did not observe.
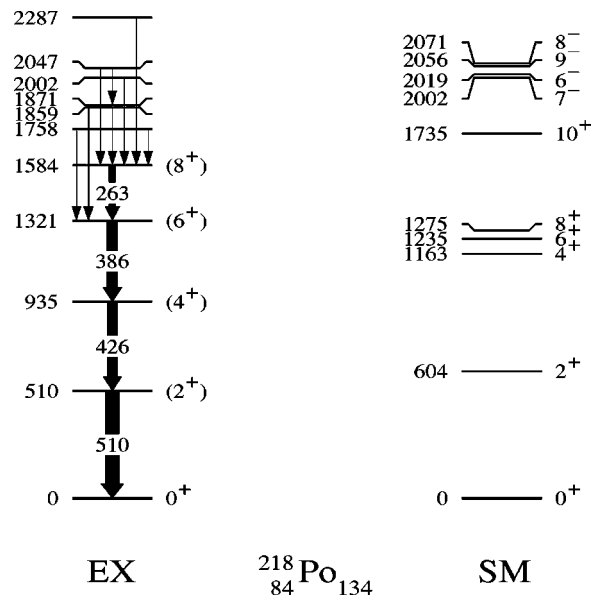

FIG. 6. Experimental (left) and calculated (right) level scheme for ^{218}Po.

Note that a downsloping $7/2^-$ proton state may also play an important role in the odd bismuth isotopes. This state is not necessarily of $\pi f_{7/2}$ origin, as it could equally be a $\pi h_{9/2} \nu g_{9/2}^2$ threequasi particle state, as frequently observed in other shells.

Allowed GT transitions to ^{218}Po are possible from $\nu i_{11/2}$ to $\pi i_{13/2}$ about 1 to 1.5 MeV above the 8^+ state but are configuration hindered. Indeed, $\nu i_{11/2}$ is less filled than $\nu g_{9/2}$ and $\pi i_{13/2}$ admixtures to the lowest lying odd-parity states might be small. This can explain the large log ft values.

In Fig. 6 the calculated ^{218}Po level scheme is drawn next to the experimental data. Only yrast states are shown, while there may be more states between 1.5 and 2 MeV of either parity. One observes that the energy of the 2^+ state is nearly correctly reproduced. From the trend of convergence for increasing C agreement will likely be reached for $C=5$, which, unfortunately, cannot be calculated within the present model. The calculated position of the 4^+ level lies too high and may require renormalization of the interaction. The deviation cannot be ascribed to a lack of convergence. The 6^+ and 8^+ levels seem too low. A larger model space will not be able to correct for this. However, the yrast states might not be populated in our experiment, as likely the shell-model states are two-quasi-neutron states, whereas the β decay of a two-quasi-particle $\pi h_{9/2} \nu g_{9/2}$ or $\nu i_{11/2}$ configuration will lead to two-quasi-proton states. From ^{210}Pb and ^{210}Po one knows that the pure two-neutron states are situated lower than the two-proton states and mixing will only increase the distance. As a matter of fact, the nonyrast states have to be calculated before one can properly judge the agreement.

The odd-parity daughter states that will take the FF transition strength are in the right place near 2 MeV. More of these, nonyrast, are expected.

VI. CONCLUSIONS

The β decay of ^{218}Bi has been investigated, a half-life of 33(1) s measured, and a level scheme constructed for the

[218]Po daughter. The experimental half-life is compared to self-consistent continuum-QRPA calculations and satisfactory agreement is reached if first-forbidden transitions are included. Shell-model calculations with the Kuo-Herling interaction and the NATHAN code coincide with the experimentally allowed possibilities for a 6^-, 7^-, or 8^- ground state of [218]Bi. The lower states of the observed stretched $E2$ cascade $8^+ \rightarrow 6^+ \rightarrow 4^+ \rightarrow 2^+ \rightarrow 0^+$ to the [218]Po ground state are reproduced but the upper levels may be nonyrast and as such outside the scope of the model.

The relatively low cross sections for neutron-rich bismuth, eclipsed by the huge francium yields, make it difficult to pursue further research in this region of the nuclear chart. Moreover, beyond mass 218 the half-lives of the francium isotopes become longer, rendering pulsed release of the activity ineffective. Although some improvement can be expected from higher laser ionization efficiencies, new techniques for the suppression of isobaric contaminations will therefore remain the main focus of future experiments.

[1] E. K. Warburton and B. A. Brown, Phys. Rev. C **43**, 602 (1991).
[2] N. Bijnens *et al.*, Phys. Rev. C **58**, 754 (1998).
[3] R. Julin *et al.*, Eur. Phys. J. A **15**, 189 (2002).
[4] K. Van de Vel *et al.*, Eur. Phys. J. A **17**, 167 (2003).
[5] L. Madansky and F. Rasetti, Phys. Rev. **102**, 464 (1956).
[6] E. Ruchowska *et al.*, J. Phys. G **16**, 255 (1990).
[7] M. Pfützner *et al.*, Phys. Lett. B **444**, 32 (1998).
[8] P. Van Duppen *et al.*, Nucl. Instrum. Methods Phys. Res. B **134**, 267 (1998).
[9] K. Rykaczewski *et al.*, *ENAM98 Exotic Nuclei and Atomic Masses, Bellaire, 1998*, AIP Conf. Proc. No. 655 (AIP, Woodbury, NY, 1998), p. 581.
[10] J. Kurpeta *et al.*, Eur. Phys. J. A **7**, 49 (2000).
[11] J. Kurpeta *et al.*, Eur. Phys. J. A **18**, 5 (2003).
[12] V. N. Fedosseev *et al.*, Nucl. Instrum. Methods Phys. Res. B **204**, 353 (2003).
[13] U. Koester *et al.*, Nucl. Phys. **A701**, 441c (2002).
[14] H. De Witte *et al.* (unpublished).
[15] J. Kurpeta *et al.*, Eur. Phys. J. A **18**, 31 (2003).
[16] See GEANT, http://wwwinfo.cern.ch/asd/geant
[17] K. Langanke and G. Martinez-Pinedo, Rev. Mod. Phys. **75**, 819 (2003).
[18] I. N. Borzov, Phys. Rev. C **67**, 025802 (2003).
[19] I. N. Borzov, S. A. Fayans, E. Krömer, and D. Zawischa, Z. Phys. A **355**, 117 (1996).
[20] A. B. Migdal, *Theory of Finite Fermi Systems and Atomic Nuclei Properties* (Interscience, New York, 1965).
[21] I. N. Borzov *et al.*, Sov. J. Nucl. Phys. **52**, 627 (1990); **55**, 73 (1992).
[22] P. Möller, J. R. Nix, and K.-L. Kratz, At. Data Nucl. Data Tables **66**, 131 (1997).
[23] P. Möller, B. Pfeiffer, and K.-L. Kratz, Report No. LANL-UR-02-2919, 2002.
[24] A. Staudt, E. Bender, K. Muto, and H.-V. Klapdor-Kleingrothaus, At. Data Nucl. Data Tables **44**, 79 (1990); M. Homma *et al.*, Phys. Rev. C **54**, 2972 (1996).
[25] T. Tachibana, M. Yamada, and N. Yoshida, Prog. Theor. Phys. **84**, 641 (1992).
[26] J. Wood, Phys. Rep. **215**, 103 (1992).
[27] E. Caurier, G. Martinez-Pinedo, F. Nowacki, A. Poves, J. Retamosa, and A. Zuker, Phys. Rev. C **59**, 2033 (1999); E. Caurier and G. Martinez-Pinedo, Nucl. Phys. **A704**, 60 (2002).
[28] R. Firestone, *Table of Isotopes* (Wiley, New York, 1996).